Received: 25 September 2023 | Revised: 1 December 2023 | Accepted: 26 December 2023

DOI: 10.1111/jeu.13020

Journal of Eukaryotic Microbiology | ISOP Published by the International Society of Protistologists

ORIGINAL ARTICLE

Living in the cracks: Two novel genera of Variosea (Amoebozoa) discovered on an urban sidewalk

Nicholas Fry[1] | **Gabriel A. Schuler**[1] | **Robert E. Jones**[1] | **Peter G. Kooienga**[1] | **Violet Jira**[1,2] | **Maggie Shepherd**[1] | **Alexander K. Tice**[1,3] | **Matthew W. Brown**[1]

[1]Department of Biological Sciences, Mississippi State University, Mississippi State, Mississippi, USA

[2]Mississippi School for Math and Science, Columbus, Mississippi, USA

[3]Department of Biological Sciences, Texas Tech University, Lubbock, Texas, USA

Correspondence
Matthew W. Brown, Department of Biological Sciences, Mississippi State University, Mississippi State, MS 39762 USA.
Email: matthew.brown@msstate.edu

Maggie Shepherd, University of Tennessee Health Science Center College of Medicine, Memphis, Tennessee, USA

Violet Jira, School of Journalism and New Media, University of Mississippi, Oxford, Mississippi, USA

Peter G. Kooienga, Department of Internal Medicine, Icahn School of Medicine at Mount Sinai – Elmhurst Hospital Center, Elmhurst, New York, USA

Present address
Gabriel A. Schuler, DEVCOM Army Research Laboratory, Adelphi, Maryland, USA

Funding information
United States National Science Foundation (NSF) Division of Environmental Biology (DEB), Grant/Award Number: 2100888

Abstract

Biological soil crusts represent a rich habitat for diverse and complex eukaryotic microbial communities. A unique but extremely common habitat is the urban sidewalk and its cracks that collect detritus. While these habitats are ubiquitous across the globe, little to no work has been conducted to characterize protists found there. Amoeboid protists are major predators of bacteria and other microbial eukaryotes in these microhabitats and therefore play a substantial ecological role. From sidewalk crack soil crusts, we have isolated three naked amoebae with finely tapered subpseudopodia, and a simple life cycle consisting of a trophic amoeba and a cyst stage. Using a holistic approach including light, electron, and fluorescence microscopy as well as phylogenetics using the ribosomal small subunit rRNA gene and phylogenomics using 230 nuclear genes, we find that these amoeboid organisms fail to match any previously described eukaryote genus. However, we determined the amoebae belong to the amoebozoan lineage Variosea based on phylogenetics. The molecular analyses place our isolates in two novel genera forming a grade at the base of the variosean group Protosteliida. These three novel varioseans among two novel genera and species are herein named "*Kanabo kenzan*" and "*Parakanabo toge*."

KEYWORDS
amoeba, biodiversity, microbe, phylogenetics, protist

INTRODUCTION

AN increasing global population brings an increase in urbanization, and macroscopic biodiversity is falling at an alarming rate (McKinney, 2002). Unfortunately, little is known about the impact of urbanization on the microbial world's biodiversity. While many habitats are apparently destroyed by urbanization, novel conditions for life are also created on these vast human-constructed landscapes, which may provide new niches for microbes to thrive. Thus, urban microbial biodiversity and ecology are increasingly gaining traction as a topic of study in microbial ecology (see Maritz et al., 2019; Ramirez et al., 2014). While some urban biological soils have been examined for prokaryotes and microbial eukaryotes (protists), as far as we know no work has been done to characterize the microbial residents found in the cracks in between concrete sidewalks, a unique and human-generated environment. These areas create microenvironments by providing structures that collect debris and are not readily cleansed via natural weather erosion or

human-directed cleaning activities. These cracks are often exposed to extreme solar radiation, temperature fluctuations, and rapid fluctuations between aridness and wetness. These thin (typically less than 1 cm thick) soil-like environments are filled with a complete ecological chain, including many filamentous cyanobacteria and some green algae acting as primary producers, and nematode worms along with heterotrophic protists (flagellates and amoebae) serving as the major predators (Geisen & Bonkowski, 2018). Recently, we reported this as a novel area to examine biodiversity in which we found a large diversity of corycid testate amoebae (Corycida, Tubulinea, Amoebozoa) (Lahr et al., 2019) from the urban sidewalk cracks on a university campus. From that same location and nearby locations, we report here two novel genera of Amoebozoa morphologically and phylogenetically placed in the highly diverse clade Variosea.

Upon original examination of our amoeboid isolates, we were unable to confidently identify them to any known group based on their morphology. Instead, we sequenced their transcriptomes and bioinformatically extracted their SSU rRNA genes for phylogenetic comparison in an Amoebozoan-rich tree. We determined that these species belonged to Variosea. Variosea (Cavalier-Smith et al., 2004) is a morphologically diverse clade. Amoebae within Variosea range from small amoebae (10 μm) to large reticulate plasmodia (600+ μm). Recently, Variosea was grouped with Cutosea, Archamoebea and Eumycetoza as Evosea, a major clade in Amoebozoa (Kang et al., 2017). Currently, there are 26 known lineages comprising Variosea, 9 of which are known only from environmental sequences, and 17 other named clades: *Darbyshirella*, *Ischnamoeba*, Cavosteliida, Schizoplasmodiidae, *Phalansterium*, Protosteliida, *Arboramoeba*, *Heliamoeba*, *Filamoeba*, *Flamella*, *Telaepolella*, *Dictyamoeba*, Soliformoviidae, Acramoebidae, *Multicilia*, *Angulamoeba* and the undescribed soil amoeba AND16. (Berney et al., 2015) Generally, Variosea is characterized by amoebae with flabellate and elongated forms during locomotion. Some amoebae are found with a single flagellum (e.g., *Cavostelium* and *Phalansterium*), while others possess multiple flagella (e.g., *Multicilia* spp. and *Protostelium aurantium*) (Adl et al., 2018). Most varioseans have a finely pointed subpseudopodia and at least one growth cone of microtubules (Cavalier-Smith et al., 2004). Four variosean clades (Protosteliida, Schizoplasmodiidae, Soliformoviidae, and Cavosteliida) contain at least some members that have a complex life cycle that includes amoeboid cells, stalkless cysts, and the ability to form a fruiting body from a single amoeboid cell (sporocarp) (Adl et al., 2018). Many varioseans (*Filamoeba*, Schizoplasmodiidae, *Angulamoeba*, Cavosteliida, *Ischnamoeba*, *Darbyshirella*, *Dictyamoeba*, *Arboramoeba*, *Telaepolella*, and Acramoebidae) display complex branched reticulate amoebae or multinucleated plasmodia (Berney et al., 2015). The clade *Heliamoeba* is multinucleated and possesses long branching pseudopods (Berney et al., 2015).

Here we report two novel genera of Variosea which we name *Kanabo* and *Parakanabo*. The genus *Parakanabo* is represented by one isolate, "Harn W-18-15," and the other genus *Kanabo* is represented by two isolates, "Union 16-1-3" and "MSU2-1." The morphological features of these species are visually indistinguishable from each other and do not match any previously described species that we are aware of. Phylogenetic analysis of the SSU rRNA gene and phylogenomic analysis of 230 genes with PhyloFisher (Tice et al., 2021) show with high support that these isolates form a grade of novel lineages at the base of Protosteliida in a variosean-rich phylogeny. Our isolates being morphologically indistinguishable and molecularly divergent suggests either an event of cryptic speciation or convergent evolution.

Protosteliida is characterized by the capability of forming sporocarpic fruiting bodies with a single spore, their amoebae are typically flabellate in shape with finely tapered subpseudopods (Adl et al., 2018; Shadwick et al., 2009), and one species can produce flagella (Shadwick et al., 2018). Cryptic speciation has also been found within the species complex *Protostelium mycophaga* in this group (Shadwick et al., 2018). Unlike Protosteliida, the amoebae of our isolates are elongated to somewhat limax (slug-shaped) in form, no fruiting bodies have been observed, and we were not able to induce a flagellated stage.

MATERIALS AND METHODS

Isolation and culturing

Each isolate was collected similarly, and their precise locations are listed below. Briefly, each isolate was collected by scraping dry crusty material held in between two slabs of concrete with sterile metal utensils. About 0.5 g of material was taken from each location and placed into a sterile Petri dish for transport to the laboratory. Immediately the samples were rehydrated in ~20 ml of sterile spring water (Ozarka, Texas, USA) and allowed to rehydrate for 1 h. The resulting turbid solution was drained through a 500-μm mesh sieve, and two drops (~200 μl) of this liquid solution were added onto the surface of a low nutrient agar wMY (0.002 g yeast extract, 0.002 g malt extract, 0.75 g K_2HPO_4, 15.0 g agar, and 1 liter ddH_2O) in a Petri dish. The plate was left at room temperature for 5 days to allow for amoebae to grow away from the drop location. Our isolates were identified under a compound microscope and transferred using a sterile 30-gauge platinum wire bent

into a small (ca. 500 μm) crosier-like hook. By pressing the hook onto the agar surface, a meniscus of liquid is formed which is used to lift cells then they were dragged to an area where no fungi or other eukaryotes were present. To establish a clonal culture, a single amoeboid cell was isolated and transferred to wMY agar with a food organism, *Escherichia coli* MG1655. These monoxenic cultures are maintained on wMY agar plates inoculated with *E. coli* and passed every 3 weeks. They have been deposited to the Culture Collection of Algae and Protozoa (Scotland, UK) under the accession numbers below.

Strain Union 16-1-3 of *Kanabo kenzan* gen. nov. et sp. nov. was obtained from a sample of soil crust collected from in between sidewalks in front of Colvard Student Union on the campus of Mississippi State University, Mississippi, USA Lat. 33.455292°, Long. −88.789532°, in May of 2016. Accession number MN508059.

Strain Harn W-18-15 of *Parakanabo toge* gen. nov. et sp. nov. was obtained from a sample of soil crust collected from in-between bricks on the west side of Harned Hall on the campus of Mississippi State University, Mississippi, USA Lat. 33.455558°, Long. −88.787748°, in August of 2018. Accession number OQ054990.

Strain MSU2-1 of *Kanabo kenzan* gen. nov. et sp. nov. was obtained from a sample of soil crust collected between the sidewalk and retaining wall on the west side of Harned Hall (around 100 m away from the isolation locale of Union 16-1-3) on the campus of Mississippi State University, Mississippi, USA Lat. 33.455484°, Long. −88.788456°, in August of 2019. Accession number OQ054989.

Light microscopy

A Zeiss Axioskop 2 Plus (Carl Zeiss Microimaging, Thornwood, NY) was used for all image collection and was conducted with a Canon EOS R 30.3MP full-fame mirrorless CMOS color digital camera. The images taken at 40X magnification used differential interference contrast (DIC), and the images taken at 10X magnification used brightfield. To prepare samples for light microscopy, agar culture slides were first made as previously described by Brown et al. (2012). Briefly, agar culture slides are made by melting a small block (ca. 4 mm^3) of wMY agar onto a slide underneath a coverslip. After the agar hardened, the cover slip was removed, and the agar was inoculated with amoebae and cysts from a culture plate that was flooded with liquid wMY (recipe as above without agar). Subsequently, a coverslip was added back onto the inoculated agar. All measurements were taken using ImageJ software (http://imagej.nih.gov/ij/) with the Scale Bar tools for Microscopes utility (http://image.bio.methods.free.fr/ImageJ/?Scale-Bar-Tools-for-Microscopes.html).

Attempts to induce sporocarpic fruiting and flagella production

To observe whether our isolates can form sporocarpic fruiting bodies, we took an approach as detailed in Brown et al. (2012). Briefly, an autoclaved sterilized dry piece of grass straw that was soaked in a slurry of liquid wMY and *E. coli* MG1655 was placed on an agar plate with densely growing amoebae. The straw provided the amoebae with a dead plant surface to crawl on, which is often sufficient to induce fruiting in amoebae that are capable as in Brown et al. (2012). The rationale for this test is that most protosteloid sporocarpic amoebae are observed on dead plant materials (see Shadwick et al., 2009; Spiegel et al., 2017) and most often fruit on the edges of these substrates.

To observe if our isolates can form flagella, we grew a dense culture of strains Union 16-1-3, MSU2-1, and Harn W-18-15 under liquid culture conditions in 7.5 ml of liquid wMY inoculated with *E. coli* MG1655 in 25-cm^2 aerobic tissue culture flasks (VWR, USA). For other protosteloid amoebae capable of forming flagella this is sufficient to induce flagella formation (Olive, 1964).

DNA extraction and PCR

DNA from a culture plate was extracted in 100 μl of QuickExtract (Epicenter, Madison WI, USA) following the manufacturer's recommended protocol and in accordance with Walthall et al., 2016. The SSU rDNA was amplified with universal eukaryote primers known as 30F (5′ACCTTGTTACGACTT) and 1492R (5′ACCTTGTTACGACTT 3′) and GoTaq Green Master mix (Promega). The PCR parameter for SSU-rDNA amplification, cloning, and sequencing is the same as those implemented in Tice et al. (2016) and Walthall et al. (2016).

RNA extraction

Culture plates with high amoebae density were flooded with liquid wMY to suspend the cells and were transferred to a centrifuge tube to be pelleted. The cells were centrifuged at 2000 *g* for 5 min. RNA was extracted from pelleted cells using a Direct-zol RNA MicroPrep kit (Zymo Research) following the manufacturer's recommended protocol. Pelleted cells were lysed in 300 μl of TRI Reagent and 300 μl of pure ethanol. The lysed cell mixture was passed through a Zymo-Spin IC Column at 10,000 *g*, then went through two rounds of washing and centrifugation at 10,000 *g*. Cell contents in the spin column were washed with 400 μl of Direct-zol RNA PreWash followed by 700 μl of RNA Wash Buffer, then eluted in 52 μl of nuclease-free water.

Following extraction, we used a NEBNext Poly(A) mRNA Magnetic Isolation Module (New England BioLabs) to select for eukaryotic mRNA, following the manufacturer's recommended protocols. Included in the protocols for poly(A) selection is the purification of the mRNA. Briefly, NEBNext Magnetic Oligo d(T) Beads were treated with RNA binding buffer. 50 µl of these treated beads were then mixed with 50 µl of the purified RNA. The mixture was incubated at 72°C for 5 min to denature the RNA and facilitate the binding of poly-A-RNA to the beads, then allowed to incubate at room temperature for 10 min with mixing to allow the RNA to bind to the beads. The beads were then pelleted on a magnetic stand and washed twice with 200 µl of Wash Buffer to remove unbound RNA. Then we added 50 µl of Tris Buffer and incubated at 80°C for 2 min, then 25°C to elute the poly-A RNA from the beads. RNA was then rebound to the beads by adding 50 µl of RNA binding Buffer and allowed to incubate off the magnetic stand at room temperature for 10 min. The beads were then pelleted on a magnetic stand and washed twice with 200 µl of Wash Buffer. Finally, the selected mRNA was eluted from the beads by adding 17 µl of Tris buffer and incubating at 80°C for 2 min, then at 25°C, then by repelleting the beads and transfer the supernatant. The supernatant contained the desired mRNA, which was transferred to a clean tube.

Illumina library preparation

Purified mRNA was reverse transcribed to cDNA following Smart-seq2 (Picelli et al., 2014) excluding the lysis step because the starting material was mRNA from our own extraction methods (detailed above) rather than a single cell. The resulting cDNA libraries were prepared for sequencing on the Illumina platform using a Nextera XT DNA Library Preparation Kit following manufacturer protocols. The Nextera XT libraries were pooled with other libraries from organisms for unrelated studies and sequenced on an Illumina HiSeq 4000 instrument at Génome Québec (Montréal, Canada) or Psomagen (Rockville, MD, USA).

Transcriptome assembly

Adaptors, primer sequences, and low-quality bases were removed from the raw sequencing reads using Trimmomatic v. 0.36 with the options ILLUMINACLIP 2:30:10 SLIDINGWINDOW:4:5 LEADING:5 TRAILING:5 MINLEN:25 (Bolger et al., 2014). The surviving reads were assembled using Trinity v. 2.8.5 (Grabherr et al., 2011).

Molecular phylogenetics

We bioinformatically extracted small subunit rRNA gene sequences from the transcriptomes of our isolates to build single gene trees. To do so, we created a BLAST database from each assembled transcriptome of our isolates and queried a known SSU rRNA gene sequence against them. This produced SSU rRNA gene sequence hits from our isolates that we used in further analysis.

Small subunit rRNA gene sequences from our strains were included with 96 other variosean SSU rRNA gene sequences retrieved from GenBank (Clark et al., 2015) and were aligned using MAFFT with the L-INS-i algorithm (Katoh & Standley, 2013). Three Centramoebia SSU rRNA sequences from GenBank were used as an outgroup. The aligned sequences were then trimmed with BMGE software with the global entropy parameter -g 0.7. The final dataset was visually inspected for alignment errors and contained 1267 unambiguously aligned characters. The maximum likelihood tree of SSU rRNA was built from RAxML v. 8.2.12 (Stamatakis, 2014) with GTRGAMMA model of nucleotide substitution.

We performed Bayesian analysis on our final dataset to corroborate the maximum likelihood tree using MrBayes v3.2.7a under the GTRGAMMA model of substitution (Ronquist et al., 2012). The analysis ran for 20 million generations. We determined a burnin of 7,071,000 generations as the average standard deviation of split frequencies stabilized under 0.0203.

Additionally, we measured uncorrected pairwise distances between the SSU rDNA genes of our isolates using a custom python script. The three SSU rDNA sequences were first aligned to one another using MAFFT with the L-INS-i algorithm. The ends of the sequences were then trimmed to end at the same base. From the resultant alignment (available from FigShare https://doi.org/10.6084/m9.figshare.24492526.) uncorrected pairwise distances were calculated using the custom script (calculatedistances.py, https://github.com/socialprotist/calculatedistances.py/).

Molecular phylogenomics

First, proteins were predicted from the assembled transcriptomes using TransDecoder v. 5.0.0 (https://github.com/TransDecoder/TransDecoder/). From these predicted protein sequences, we queried 240 housekeeping genes using PhyloFisher (Tice et al., 2021). PhyloFisher allows us to assemble a phylogenomic dataset from our isolates and a curated database using these 240 housekeeping genes and identify probable orthologs and contaminants by manual parsing of single gene trees. The curated PhyloFisher dataset includes taxa representing the full known diversity of eukaryotes. From our isolates, we recovered orthologs from 230 genes covering

73,839 sites, which were concatenated with orthologs from the other taxa in the PhyloFisher dataset into a multigene matrix. This matrix was used as input to generate a phylogenomic tree using IQTree2 (Minh et al., 2020). First, a starting tree was inferred under the LG+G4+F+C20 site heterogeneous model of evolution. Using this tree as a guide, we inferred another tree under the LG+G4+F+C60 site heterogeneous model of evolution with posterior mean site frequencies (PMSF). Using the PSMF tree, we inferred a final maximum likelihood (ML) tree under LG+G4+F+C60+PSMF model, with 115 real bootstrap replicates.

Confocal staining and imaging

For a full step-by-step protocol for tubulin, actin, and DNA staining confocal microscopy of amoeboid organisms, see (Brown, 2019). Briefly, a primary antibody for alpha-tubulin monoclonal (Life Tech | 32-500) and secondary antibody of goat anti-Mouse IgG (Life Tech | A-11032) were prepared according to the manufacturers' protocols. Next, an agar block dense with amoebae was carefully excised from the isolate culture plate. This block was turned upside down and placed onto a culture slide (Lab-Tek™ II Chamber Slide – Thermo Scientific – 154461). Next, in 500 µl of liquid media, cells were settled and adhered to a Culture slide before the agar block was removed, and liquid media was aspirated. Cells were fixed in −80°C 100% methanol to the glass surface of the chamber slide for 2 min at room temperature. Cells were rinsed with PBS buffer three times and for 3 min each. Premade 1X BSA blocking buffer (Bovine serum albumin, Sigma-Aldrich|A4949) was applied for 10 min at room temperature. A diluted (1:500) primary antibody was added to each chamber followed by 500 µl of PBS a total of four times for 3 min per wash. The secondary antibody (1:1000) was then added for 45 min at room temperature. Cells were labeled with ActinGreen 488-nm ready probes (Life Tech | R37110) followed by NucBlue ReadyProbes (Life Tech | R37605). Cells were washed again with PBS three times for 3 min, and then cells were labeled with Fluoromount-G (Life Tech | 00-4958-02). Cells were visualized with an inverted confocal microscope (Leica TCS SPE-II) equipped with four solid state lasers (405, 488, 532/561, 635 nm excitation), under an Advanced Correction System (ACS) 63x-Oil (NA 1.30) objective controlled by the LAS X Leica software.

Transmission electron microscopy (TEM)

For TEM, amoeboid and cyst cells of *Kanabo kenzan* strain Union 16-1-3 were grown on wMY agar plates until they reached a dense culture stage. Afterward, 2–3 ml of liquid wMY was poured over the agar plate. Subsequently, cells were scrapped off and collected in sterile 15-ml falcon tube. For liquid amoeboid cultures, cells were scrapped off and collected in sterile 15-ml falcon tube. The cells were centrifuged at 4360 *g* at 4°C for 2 min to pellet the cells. The cell pellet was suspended in a cocktail of culture media containing 2.5% v/v glutaraldehyde and 1% osmium tetroxide and fixed for 30 min on ice. The fixed cells were centrifuged again at 4360 *g* at 4°C for 1 min to pellet the cells again. The cell pellet was then washed with wMY liquid and then washed twice with distilled water. Cells were concentrated again by centrifugation at 4360*g* and embedded in 2.0% (w/v) agar prepared with distilled water. Agar blocks were dehydrated through an ethanol series (25%, 50%, 75%, 100%) and embedded in SPI-Pon 812 Epoxy resin (SPI Supplies, West Chester, PA). Sections 60–70 nm thick were cut on a Reichert ultramicrotome mounted on a pioloform film in grids using a diamond knife and stained with saturated uranyl acetate in 50% ethanol and lead citrate. Sections were observed using a JEOL 1230 120 kV TEM (Institute for Imaging & Analytical Technologies, Starkville, MS).

Scanning electron microscopy (SEM)

For SEM, amoeboid and cyst cells of *Kanabo kenzan* isolates "Union 16-1-3" and "MSU2-1" were grown on wMY agar plates until they reached a dense culture stage. Coverslips were then prepared by coating with poly-L-lysine to aid in the adhesion of amoebae to the coverslip. Coverslips were submerged in poly-L-lysine for 5 min, then removed and allowed to air dry overnight. A drop of sterile liquid wMY was added to a coated coverslip, then a small (5 mm^2) block of agar was cut from an area of high amoebae density and placed cells down in the liquid on the coverslip. Amoebae were allowed to transfer from the agar block to the surface of the coverslip for 1 h. The agar blocks were then removed, and the coverslips were inverted inside a closed center-well culture plate over 3 drops of 4% osmium tetroxide for 15 min inside of a fume hood to vapor fix the amoebae cells. Afterward, the coverslips were rinsed with sterile water four times, then placed face up. Cells on the coverslips were dehydrated through an ethanol-water series (25%, 50%, 75%, 100%), each step lasting 15 min. Cells on the coverslips were then dried through an HMDS-ethanol series (25%, 50%, 75%, 100%), each step lasting 15 min. Finally, excess HMDS was removed, and the cells were allowed to air dry overnight, without the use of a critical point drier. Coverslips were affixed to metal SEM stubs with carbon tape and coated with 20 nm of platinum using a EMS150T Turbo-Pumped Sputter Coater. Cells on coverslips were observed using a JEOL 6500 10-kV SEM (Institute for Imaging & Analytical Technologies, Starkville, MS).

RESULTS

General morphology of isolates

Our three isolates are morphologically indistinguishable from each other, so we provide a common description here. Micrographs of each isolate are provided individually, as well as morphometrics. Each isolate was obtained from soil crust in-between sidewalk slabs and maintained on wMY agar plates. We observed a trophozoite stage (Figures 1A–F,H,I, 2A–C,G, and 3A–D) and a dormant cyst stage (Figures 1F,G, 2D–F, and 3E–G) of our isolates. Our isolates do not have a permanent locomotive organelle such as a flagellum.

Our isolates can form various morphologies, including irregular compact shapes in a dense area or when emerging from encystment (Figures 1A, 2A, and 3A). When amoebae begin to crawl away from dense areas the locomotive form is characteristically limax (i.e., slug shaped) with finely tapered subpseudopodia, displaying an elongated hyaloplasm and a posterior contractile vacuole (Figures 1B–E, 2B,C, and 3B–D). Under light microscopy the finely tapered subpseudopodia on our isolates appear to be tapering and finely tipped. When a cell is advancing, we notice a gentle bulge of hyaloplasm which covers one fifth to one half of a cell area (Video S1). We also observed a uroid with short trailing finely tapered subpseudopods at the posterior end (Figures 1E, 2C, and 3D). All isolates appeared uninucleate under light microscopy, both while locomotive and encysted (Figures 1B–G, 2B–E, and 3B–G). The nucleolus is visible inside the nucleus (Figures 1D,F, 2C,E, and 3D,F). The nucleolus shape is circular at most times but sometimes amorphous. We did not observe any eruptive or rapid movement, nor any discernable glycocalyx or scaly features on the cell membrane.

To study the distribution of microtubules, actin, and DNA, cells from isolate "Union 16-1-3" were labeled with NucBlue (DNA), Fluoromount G probes (tubulin), and ActinGreen probes (actin). Actin filament was seen across the whole cell and was more intensely localized at the posterior end (Figure 4B). DNA was localized in the middle of the cell, where the nucleus was generally seen in light microscopy (Figure 4A). We also noticed that microtubules were localized near the

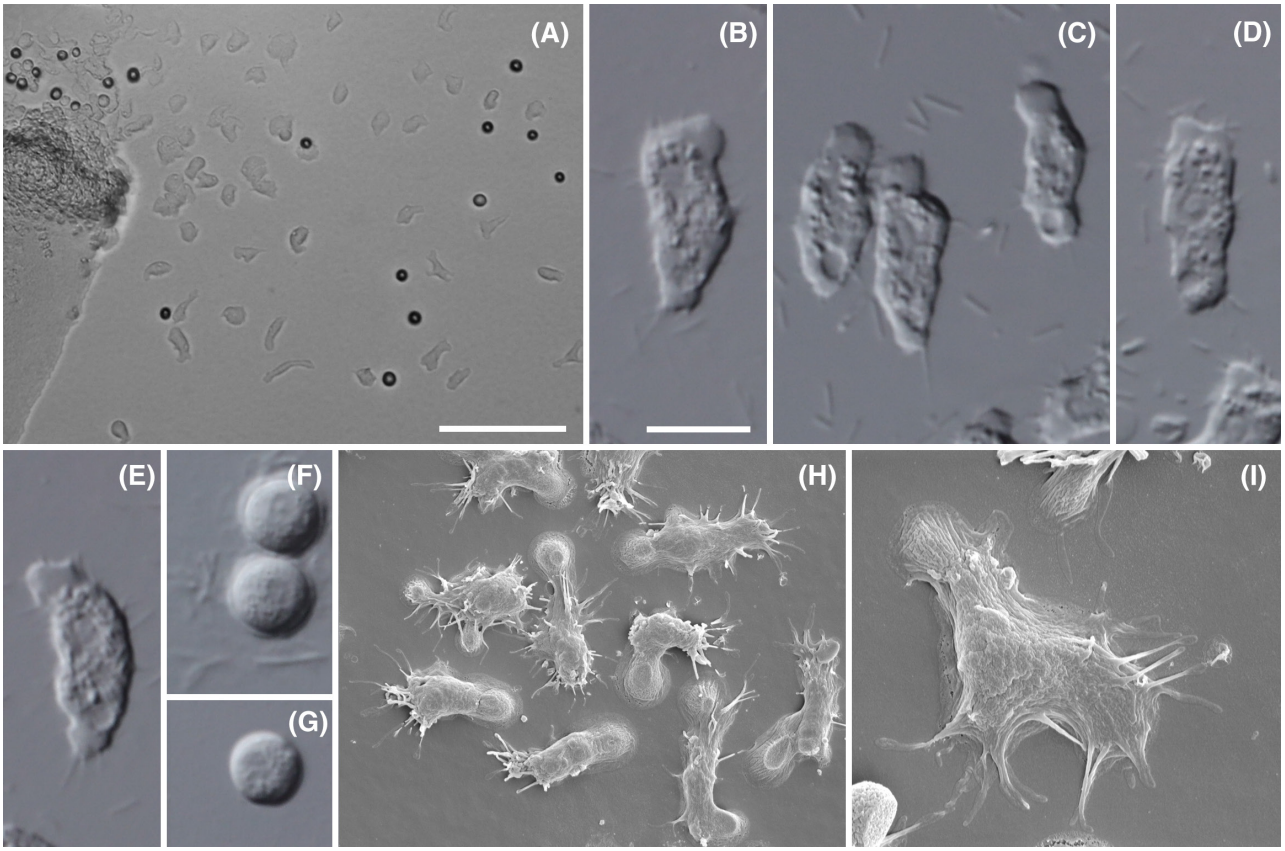

FIGURE 1 Light and scanning electron micrographs of *Kanabo kenzan* sp. nov., strain Union 16-1-3. (A) Diversity of trophic forms and cysts on the surface of an agar plate, scale bar = 100 μm; (B and C) Trophic cells, showing tubular form, subpseudopodia, and anterior locomotive hyaloplasm, scale bar = 10 μm (B–G to scale); (D) Trophic cell with nucleus and nucleolus visible in center of cell; (E) Trophic cell with distinct uroid and trailing finely tapered subpseudopods; (F and G) Encysted amoebae; (H) SEM image of many trophic amoebae with distinct finely tapered subpseudopods and uroids, 3000X magnification, scale bar = 10 μm; (I) SEM image of single trophic amoebae, 7500X magnification, scale bar = 5 μm.

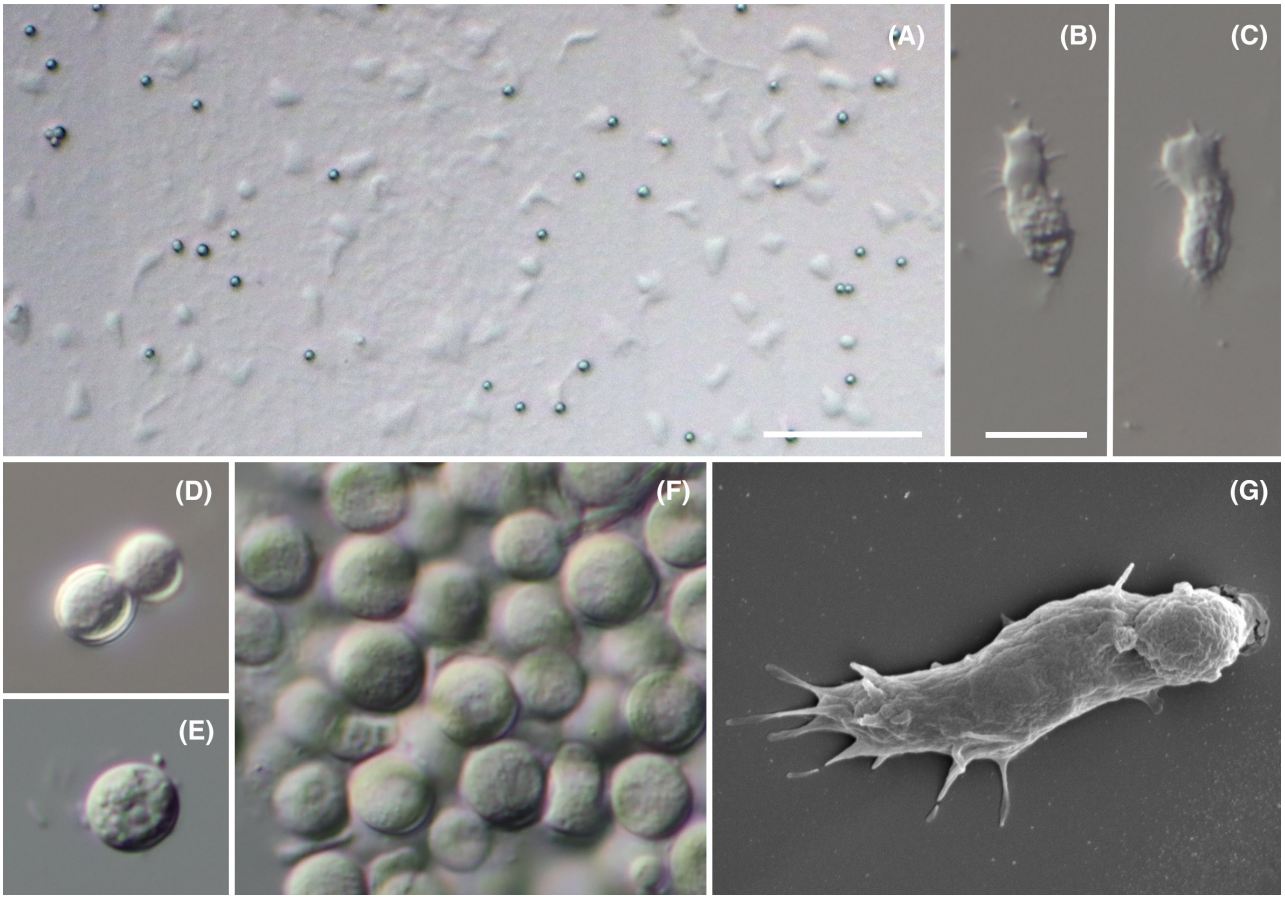

FIGURE 2 Light and scanning electron micrographs of *Kanabo kenzan* sp. nov., strain MSU2-1. (A) Diversity of trophic forms and cysts on the surface of an agar plate, scale bar = 100 μm; (B and C) Trophic cells, showing tubular form, finely tapered subpseudopodia, anterior locomotive hyaloplasm, and nucleus and nucleolus, scale bar = 10 μm (B–F to scale); (D and E) Cysts with nucleus visible; (F) Cluster of cysts; (G) SEM image of a single trophic amoeba, 10,000X magnification, scale bar = 3 μm.

nucleus (Figure 4C). This area could be interpreted as the location of the microtubule organizing center (MTOC), especially near the nucleus (Figure 4D). Similarly, the sister clade to our isolates, Protosteliida, have microtubule organizing centers located near the nucleus (Spiegel et al., 1994).

Food vacuoles were invisible under the light microscope but are visible in TEM images of cells of isolate "Union 16-1-3" (Figure 5C). Electron microscope micrographs clearly show tubular cristae in an ovoid mitochondrion (Figure 5B). The plasma membrane appeared to be smooth (Figure 5B,C). We also noticed possible pink pigments in (perhaps lipid) droplets in cysts (Figure 5A).

Morphometrics

Morphometric data for each isolate were obtained from light micrographs at 40X magnification while amoebae were in a locomotive stage and while encysted. We observed limax locomotive amoebae and round smooth-walled cysts of each isolate. We measured the lengths and widths of trophic amoebae, as well as the diameter of their nuclei and nucleoli. Since the cysts were round and smooth, we measured only their diameter. Summaries of the data obtained for each isolate are shown in Table 1.

SSU rRNA gene phylogenetic analyses

The SSU rRNA gene phylogenies consisting of representative taxa of all amoebozoan groups indicated that our isolates group with variosean taxa (data not shown). As a result, we constructed a phylogenetic tree focused on Variosea (Figure 6) with Centramoebia as an outgroup. The phylogenetic analysis of Variosea as inferred from a maximum likelihood tree of the SSU rRNA gene recovers the novel isolates in two clades of Variosea as a grade at the base of Protosteliida with medium to high bootstrap values in ML.

Pairwise distance measurements between our isolates shows that Union 16-1-3 and MSU2-1 differ in only three sites, while isolate Harn W-18-15 differs by 222 sites from Union 16-1-3. This results in a 12.22% difference between the SSU rRNA gene of *Parakanabo toge* and *Kanabo kenzan*.

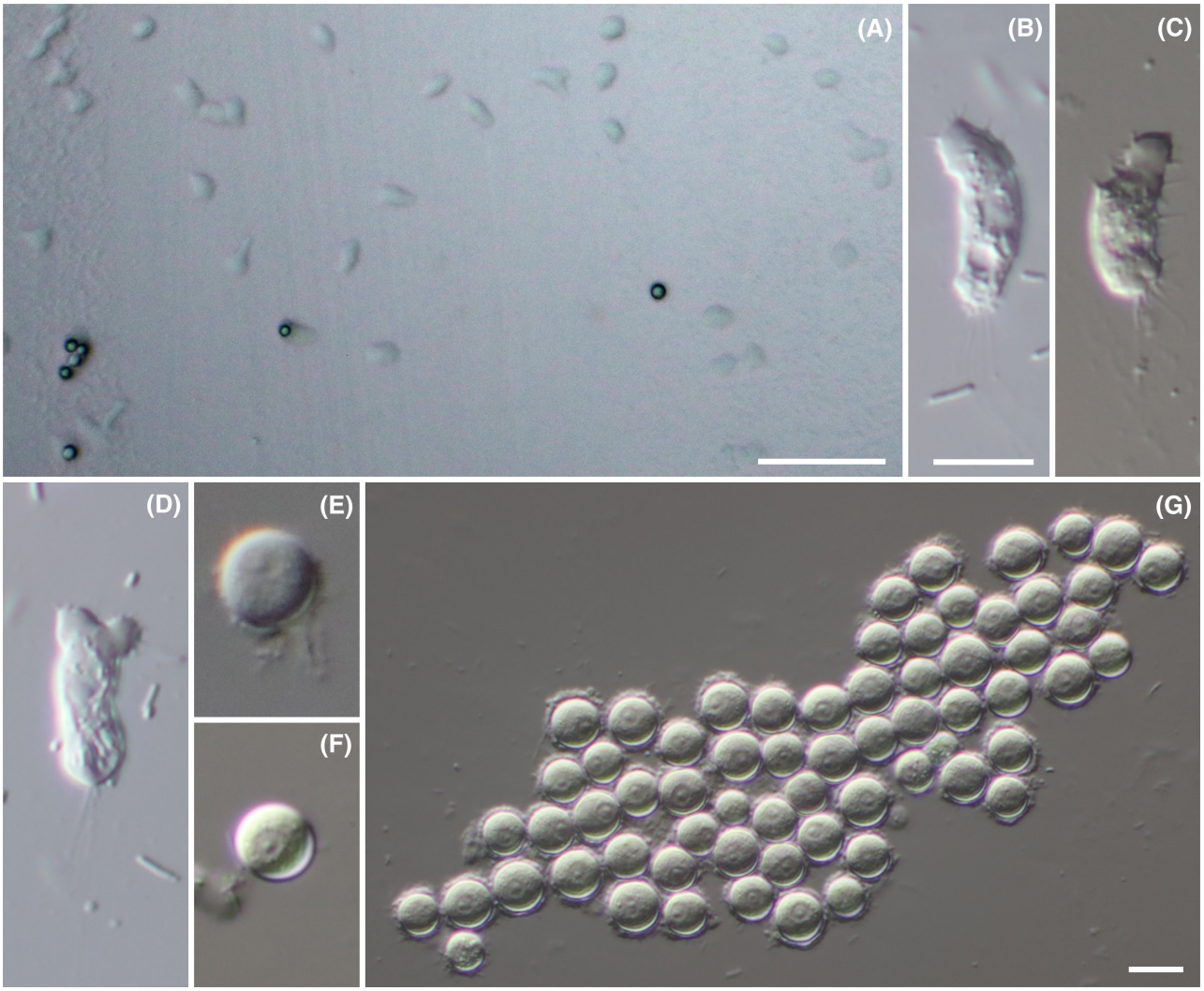

FIGURE 3 Light micrographs of *Parakanabo toge* sp. nov., strain Harn W-18-15. (A) Diversity of trophic forms and cysts on the surface of an agar plate scale bar = 100 μm; (B and C) Trophic cells, showing tubular form, finely tapered subpseudopodia, anterior locomotive hyaloplasm, and trailing filopodia, scale bar = 10 μm (B–F to scale); (D) Trophic cell with nucleus visible at its center; (E and F) Cysts with nucleus and nucleolus visible; (G) Cluster of cysts, scale bar = 10 μm.

Additionally, the SSU rRNA gene phylogeny shows *Schoutedamoeba minuta* falling outside of the known diversity of Variosea with full support from both ML and Bayesian analysis.

Phylogenomic analyses

In addition to our phylogenetic analyses using the SSU rRNA gene, we used PhyloFisher (Tice et al., 2021) to build a phylogenomic dataset from transcriptomic data. Using PhyloFisher, we gathered 230 genes, totaling 73,839 sites, to form a concatenated matrix from those genes. This concatenated matrix was used for phylogenomic analyses to increase resolution of deep branches and obtain a more robust phylogeny (Figure 7). The genera *Kanabo* and *Parakanabo* are fully supported as distinct groups by this analysis. As in the SSU rRNA gene phylogenies, the phylogenomic analyses illustrate that our new isolates are paraphyletic of one another, with Union 16-1-3 and MSU2-1 grouping together. Additionally, the topology of the tree, including the deep branches, matches previous phylogenomic analyses of Amoebozoa (Kang et al., 2017) to the exclusion of the Tevosa clade from Kang et al., 2017 previously demonstrated in Tice et al. (2023) and Tekle et al. (2022). Rather in our analyses and these latter studies Evosea groups with Discosea.

DISCUSSION

As human populations increase, natural landscapes are bound to be urbanized. This can lead to changes in the composition of biodiversity, ecology, and communities of microorganisms. A tiny crack between the concrete slabs of a sidewalk becomes a surprising hot spot for biodiversity. These soil-water crusts are potentially a

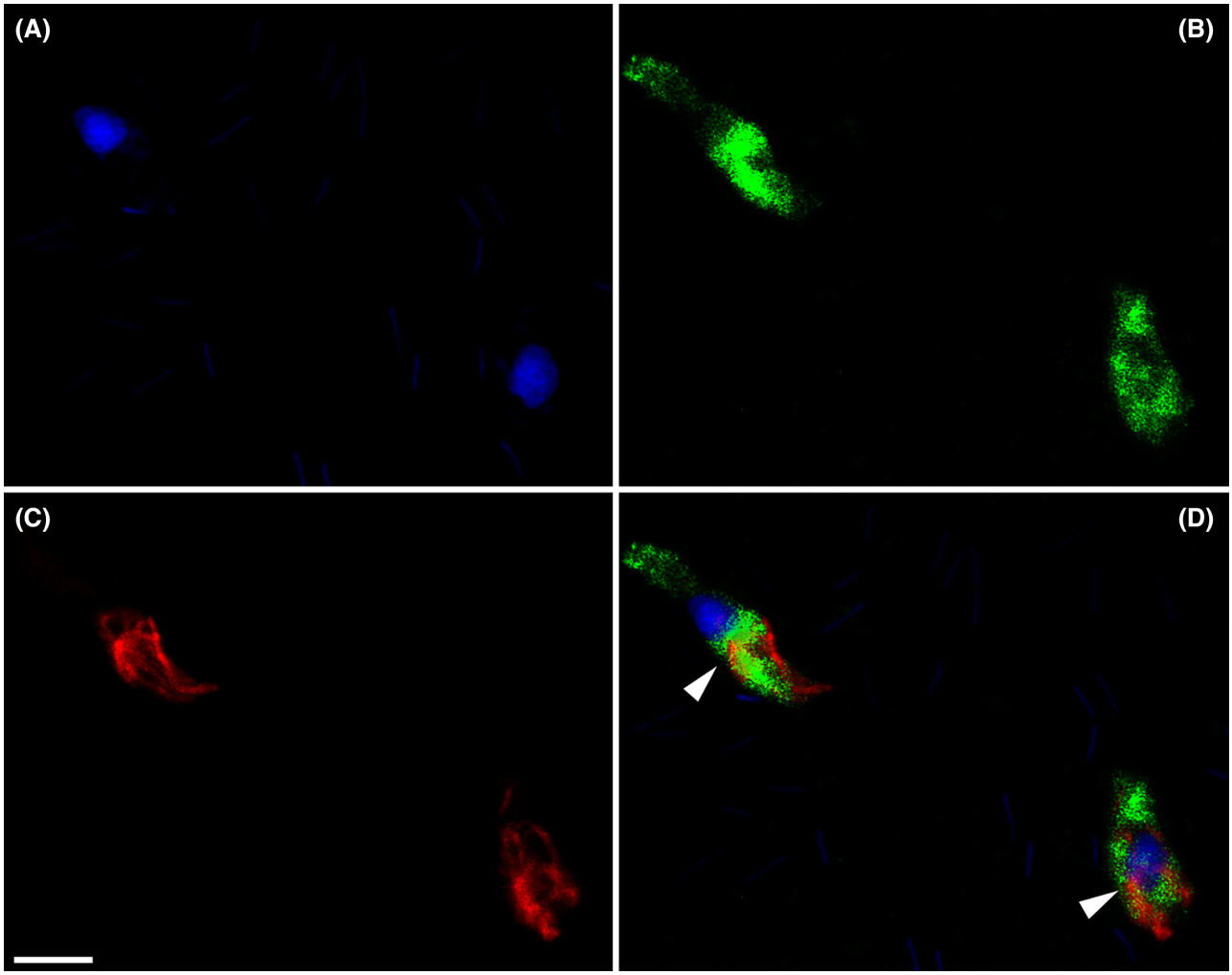

FIGURE 4 Histocytochemical and Immunofluorescence localization of cellular structures of *Kanabo kenzan* (Union16-3-1) amoebae using confocal microscopy. (A) DNA (blue), scale bar = 5 μm (A–D to scale); (B) Actin (green); (C) Tubulin (red); (D) Co-localization of DNA, Actin, and tubulin markers. Arrows indicate higher intensity localization of tubulin near the nucleus.

treasure trove for undiscovered protists as we demonstrate through the identification of two novel lineages of amoeboid organisms isolated from these environments.

These isolates are visually indistinguishable and display the following morphological characteristics: limax locomotion, finely tapered subpseudopodia, elongated hyaloplasm, a posterior contractile vacuole, and a small round cyst stage. This particular combination of morphological traits stood out, because it does not match any species of amoeboid protist of which we were aware. However, these morphological characters are few in number and vague in designation, making the isolates difficult to place taxonomically based on morphology alone. For example, limax body plans are present in all major groups of Amoebozoa: Tubulinea (Smirnov et al., 2011), Discosea (Blandenier et al., 2017; Kudryavtsev et al., 2022; Volkova & Kudryavtsev, 2021), and Evosea (Wichelen et al., 2016), as well as the amoeboid Excavate group Heterolobosea. Despite the presence of similar limax shapes in Heterolobosea, our amoebae lacked the characteristic eruptive movement of heterolobosean amoebae, which is a diagnostic morphological character strongly supported by molecular studies (Harding et al., 2013; Nikolaev et al., 2004). Because of this, we were confident that our isolates belonged in Amoebozoa.

Among the major groups of Amoebozoa each one contains at least one group with limax movement. The group Tubulinea is the one classically characterized by amoebae able to form limax shapes (Smirnov et al., 2011). Until recently it was thought that the limax body plan in Amoebozoa was a synapomorphy of Tubulinea and unique to the group among the Amoebozoans (Kudryavtsev et al., 2022). However, both Discosea and Evosea now contain species displaying limax locomotion. Three newly characterized limax amoebae, *Coronamoeba villafranca* (Kudryavtsev et al., 2022), *Janickina pigmentifera* (Volkova & Kudryavtsev, 2021), and *Mycamoeba gemmipara* (Blandenier et al., 2017) have been shown to belong in Discosea. Additionally, *Schoutedamoeba minuta* potentially belongs in Evosea (Wichelen et al., 2016).

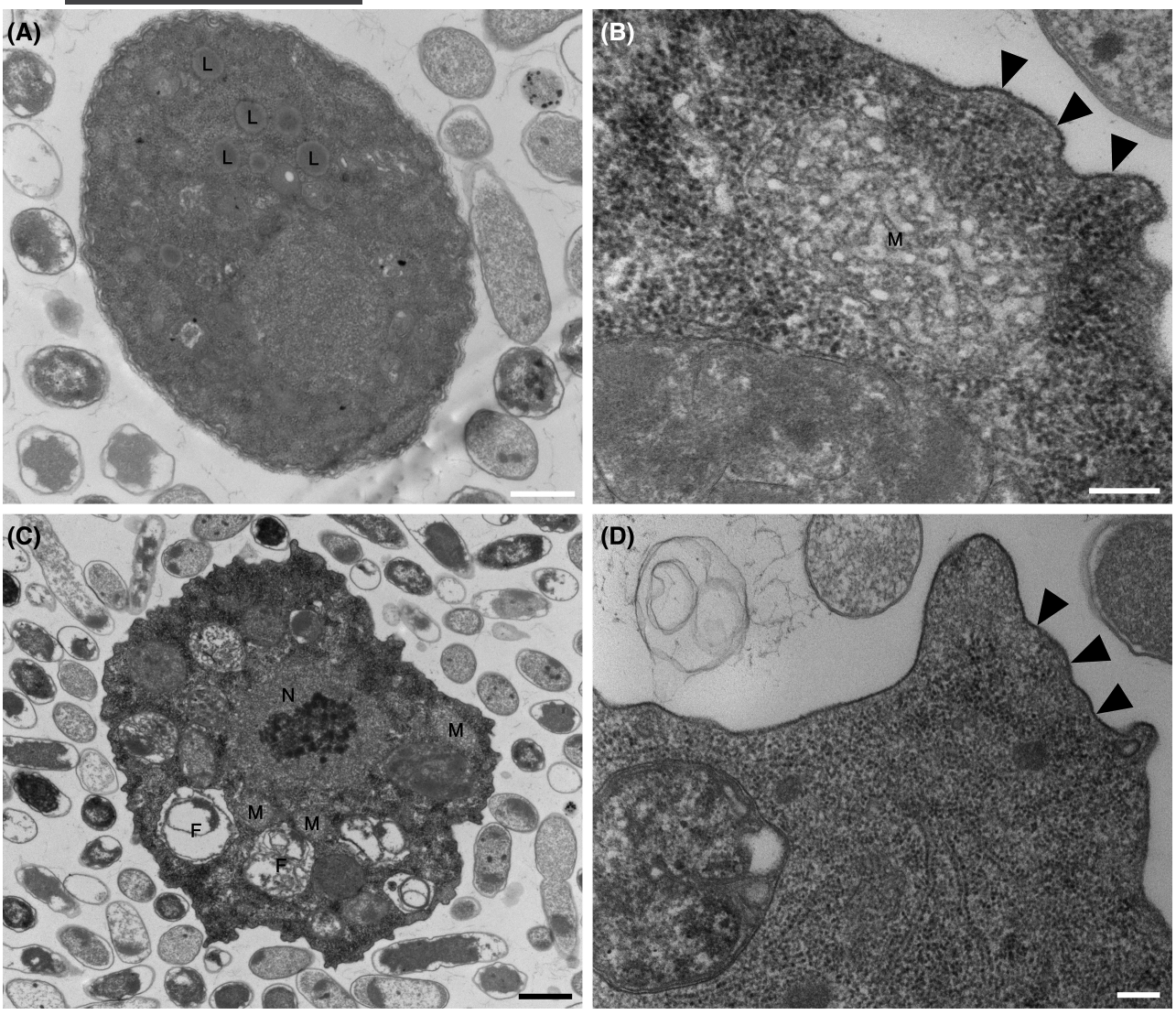

FIGURE 5 Transmission electron micrographs of *Kanabo kenzan* sp. nov., strain Union 16-1-3. (A) Cyst showing lipid droplets (L), scale bar = 600 nm; (B) Amoeba with mitochondria (M), arrows indicate plasma membrane of amoeboid cell, scale bar = 200 nm; (C) Amoeba showing nucleus (N), and nucleolus, mitochondria (M), and food vacuoles (F), scale bar = 1 μm; (D) Amoeba that shows enlarged plasma membrane, indicated by arrows, scale bar = 200 nm.

Additionally, finely tapered subpseudopodia are not diagnostic of a single major group of Amoebozoa. Two major groups of Amoebozoa contain taxa with finely tapered subpseudopodia. This characteristic is most common to Variosea in Evosea (Berney et al., 2015), but is also present in three Tubulinid groups: Echinamoebida (Cavalier-Smith et al., 2004), Leptomyxida (Smirnov et al., 2017), and Phryganellina (Griffin, 1972).

Based on the prominent morphological characters alone, we could not confidently identify our isolates to any major group of Amoebozoa. Consequently, we turned to molecular phylogenetic analyses to identify our isolates. We first built a Maximum Likelihood SSU rRNA gene tree with our isolates and 96 other variosean SSU rRNA sequences, consisting of 1267 sites, representing the full known diversity of Variosea. We corroborated the Maximum Likelihood tree with Bayesian analysis, which yielded a nearly identical tree topology. This SSU rRNA gene tree revealed that our isolates form a moderately supported grade at the base of the group Protosteliida (Figure 6), but did not provide sufficient support for a satisfying exact branching order.

We continued by performing an Amoebozoa-wide phylogenomic analysis using 230 genes with 73,839 amino acid sites to resolve the exact branching order of our isolates and the deeper relationships surrounding them (Figure 7). Our multigene dataset also highly supports our isolates forming a grade at the base of Protosteliida.

In both single-gene and multigene phylogenies our isolates form two separate genera-level clades, indicating a high degree of genomic divergence. The isolates "Union 16-1-3" and "MSU2-1" group together in the novel genus and species we name *Kanabo kenzan*, and the

Journal of Eukaryotic Microbiology ISOP Published by the International Society of Protistologists

TABLE 1 Summary of morphometric data for each isolate, including range of measurements, average measurements, standard deviation, and sample size.

	Mean	Standard deviation	Minimum	Maximum	Sample size
Kanabo kenzan isolate Union 16-1-3					
Cell length	13.2 μm	2.4 μm	7.9 μm	15.8 μm	101
Cell width	6.8 μm	1.8 μm	3.8 μm	9.6 μm	101
Nucleus diameter	2.9 μm	0.8 μm	1.7 μm	5.1 μm	88
Nucleolus diameter	1.6 μm	0.4 μm	0.6 μm	2.6 μm	88
Cyst diameter	7.2 μm	1.2 μm	4.9 μm	9.1 μm	62
Kanabo kenzan isolate MSU2-1					
Cell length	14.9 μm	2.7 μm	8.0 μm	22.3 μm	178
Cell width	5.9 μm	0.9 μm	3.9 μm	8.4 μm	178
Nucleus diameter	2.7 μm	0.4 μm	1.8 μm	3.8 μm	51
Nucleolus diameter	1.6 μm	0.3 μm	1.1 μm	2.4 μm	51
Cyst diameter	8.0 μm	0.6 μm	6.8 μm	8.7 μm	20
Parakanabo toge isolate Harn W 18 15					
Cell length	18.9 μm	3.1 μm	10.2 μm	29.3 μm	63
Cell width	6.5 μm	1.1 μm	4.2 μm	9.1 μm	63
Nucleus diameter	3.8 μm	0.7 μm	2.3 μm	5.5 μm	20
Nucleolus diameter	2.1 μm	0.6 μm	1.2 μm	3.3 μm	20
Cyst diameter	8.5 μm	0.6 μm	7.6 μm	9.9 μm	20

Note: For individuals of each isolate, we measured cell length, cell width, nucleus diameter, nucleolus diameter, and cyst diameter.

isolate "Harn W-18-15" groups in the other novel genus and species we name *Parakanabo toge*.

Kanabo kenzan and *Parakanabo toge a*re morphologically identical as seen in Figures 1–3, yet they show considerable genetic divergence as seen in Figures 6 and 7. This discrepancy indicates either an event of cryptic speciation or convergent evolution (Mann & Evans, 2008). Cryptic speciation has been documented across the tree of Eukaryotes, including Amoebozoa, with cases occurring in clades in close proximity to our isolates (Shadwick et al., 2018; Tice et al., 2016). Such events are unsurprising for amoeboid organisms given their relatively few morphological characteristics. In the case of *Protostelium*, Shadwick et al. (2018) found many amoebae species with identical fruiting behavior and trophic morphology, but one species, *Protostelium* (previously *Planoprotoselium*) *aurantium*, could form flagella in liquid culture. In the group Centramoebia, Tice et al. (2016) found that two groups with identical trophic amoebae, *Acanthamoeba* and *Protacanthamoeba*, are separated by morphologically dissimilar taxa, including taxa with complex behavior (Tice et al., 2016). In these organisms with a scarcity of morphological traits, evolutionary convergence can appear deceptively parsimonious, at least from the perspective of light microscope observation. However, without more taxa between or surrounding *Kanabo* and *Parakanabo*, it is currently impossible to determine whether they are cryptically speciose or converged independently on their identical morphology.

Transmission electron micrographs of *Kanabo kenzan* isolate "Union 16-1-3" revealed ultrastructure supporting the results of our phylogenetic analysis. *Kanabo kenzan* possesses tubular mitochondrial cristae as seen in Figure 5B. This mitochondrial architecture is characteristic of nearly all Amoebozoan lobose amoebae, as opposed to the discoidal mitochondrial cristae found in Heterolobosean amoebae (Pánek et al., 2020). Cells of *Kanabo kenzan* also contain what appear to be lipid droplets in their granuloplasm (Figure 5A). These lipid droplets are shared by the group Protosteliida, which agrees with the phylogenetic placement in proximity to this group (Spiegel et al., 1994).

Histocytochemical and immunofluorescence images also revealed a potentially pertinent feature supporting the phylogenetic placement of *Kanabo kenzan*. The stained tubulin localizes to a microtubule organizing center (MTOC) associated with the nucleus (Figure 4D). Nucleus-associated MTOC's are also shared by the group Protosteliida (Spiegel et al., 1994).

Due to the close phylogenetic proximity of our isolates to Protosteliida, we hypothesized that they may also share some of their complex behaviors. Protosteliida amoebae are irregular circular or flabellate amoebae with finely tapered pseudopodia, except for *Protostelium aurantium* which has an amoeboflagellate stage (Shadwick et al., 2018). All species in this group are capable of

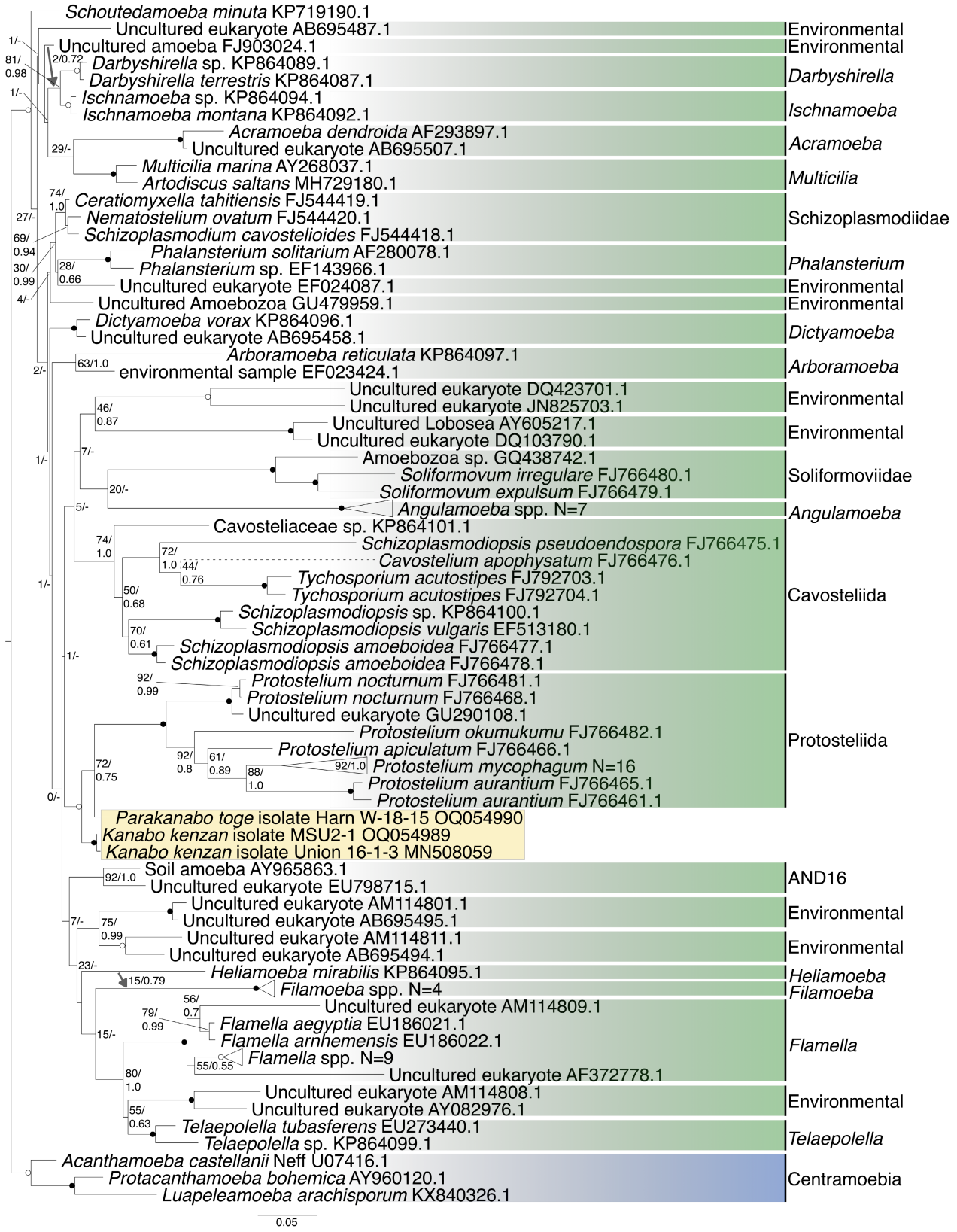

FIGURE 6 Maximum likelihood 18S SSU tree of all 26 variosean groups with Centramoebia as an outgroup, using RAxML with GTR-GAMMA model of substitution. Bootstrap support values and Bayesian posterior probabilities (see Methods) are shown at nodes where both values are below 50% or 0.75, respectively. Nodes shown as an asterisk indicate the node was not recovered by Bayesian analysis. Nodes with a black dot indicate 95% bootstrap support and a posterior probability of 1.0. Nodes with a white dot indicate greater than 50% bootstrap support and/or a posterior probability of 0.75. The gray arrow depicts a difference between the ML and Bayesian tree topologies. The *Cavostelium apophysatum* branch has been reduced by 50%, indicated by a dashed line. Our novel isolates are highlighted in yellow.

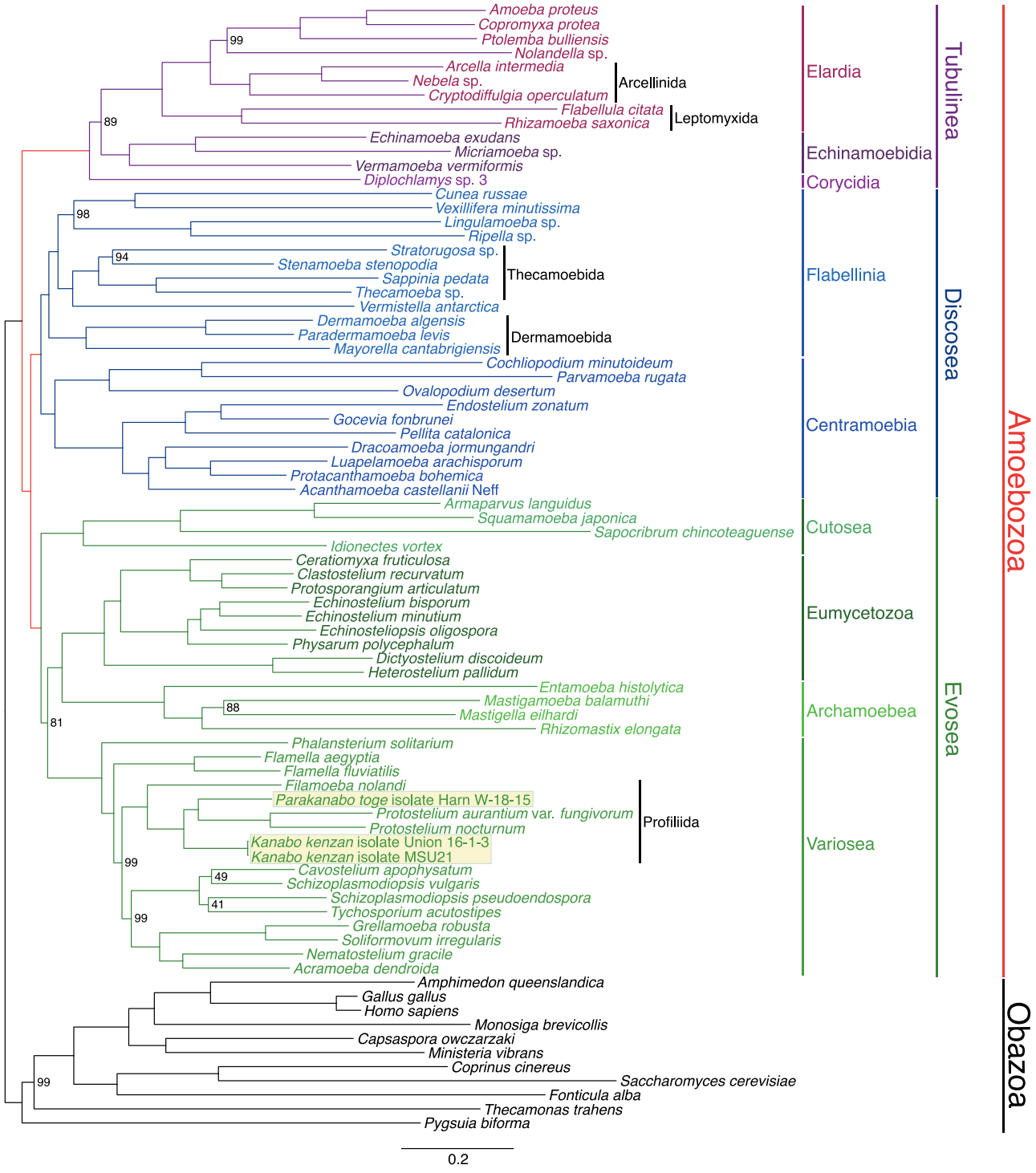

FIGURE 7 Maximum likelihood tree of Amoebozoa, using Obazoa as an outgroup, built with IQTree2 under LG+G4+F+C60+PSMF model. Constructed from a multigene concatenated matrix of 230 genes covering 73,839 total sites generated by PhyloFisher. Relevant clades are defined by labeled vertical bars, and our isolates are highlighted in yellow. The numbers at each node represent bootstrap values generated under the LG+G4+F+C60+PSMF model, and blank nodes represent full bootstrap support.

sporocarpic fruiting body formation, in which a single trophic cell becomes rounded and produces an acellular stalk to lift the cell mass from the surface of the substrate (Shadwick et al., 2018). We then tested whether we could induce sporocarpic fruiting or flagella formation in our isolates.

To test sporocarpic fruiting we introduced a piece of sterilized grass straw to each agar culture, a technique adapted from Brown et al. (2012). The rationale for adding plant matter is that protosteloid amoebae are primarily found fruiting on dead plant substrate when observed in primary isolation. We soaked the

grass in a slurry of food bacteria, *E. coli*, to promote colonization of the grass pieces. The amoebae grew well and colonized the grass pieces in each culture of each isolate, but no fruiting bodies were observed over three attempts for each isolate. However, this does not exclude our isolates' ability to make fruiting bodies. The events triggering fruiting body formation in different protosteloid amoebae are idiosyncratic. Such factors include nutrient availability, light cycles, substrate specificity, flooding, humidity, physical disturbance, pH, co-culturing, or a combination of these factors.

To attempt to induce flagella formation we grew each isolate in liquid wMY culture, as opposed to the usual agar wMY. For other flagella-forming protosteloid amoebae, specifically those found in Protosteliida, *Protostelium aurantium*, presence in liquid conditions is sufficient to induce flagella formation (Olive & Stoianovitch, 1971). Our isolates grew well in liquid wMY media through two passages over 1 month, but no flagella were observed. In contrast, amoebae of *P. aurantium* form flagella within minutes to hours when in liquid (Olive & Stoianovitch, 1971).

Kanabo kenzan and *Parakanabo toge* represent the second and third species in Evosea with limax locomotion. This further supports the nonuniformity of morphological designation in Amoebozoa (Kudryavtsev et al., 2022). Our isolates are yet another example of untapped diversity in Amoebozoa. Given Amoebozoa's great diversity of form and behavior, there is still much to be found with careful exploration of various environments. There lie novel genera just beneath our feet in places even as mundane as urban sidewalks.

TAXONOMIC SUMMARY

Amoebozoa Lühe (1913), sensu Cavalier-Smith (1998).

- Tevosa Kang et al. (2017).
- Evosea Kang et al. (2017).
- Variosea Cavalier-Smith et al. (2004).
- Profiliida Kang et al. (2017).

TAXONOMY OF NOVEL GENERA AND SPECIES

Kanabo Fry & Brown n. g

Diagnosis. A small limax-shaped amoeba, with greater length than breadth, with finely tapered subpseudopodia, generally tubular shape, oftentimes tubular shape in form, with an anterior contractile vacuole, and can form a round, smooth-walled cyst. Rarely, cells form an irregular circular shape. Amoeboid cells in locomotion display characteristics of a limax shape with elongated hyaloplasm and anterior contract vacuole. Mitochondrial cristae are tubular in cross-section.

Type species. *K. kenzan*.

ZooBank ID: urn:lsid:zoobank.org:act:8052C5B4-5070-445F-AA65-74736492FADD.

Etymology. Named after the Japanese noun, Kanabō, a feudal spiked metal club weapon. As Japanese nouns have no grammatical gender, *Kanabo* is neuter. The amoebae bear resemblance to the weapon from the posterior circle to the long shape and spiked anterior.

Kanabo kenzan Fry & Brown n. sp.

Diagnosis. Length in locomotion 7.9–15.8 µm (average 13.2 µm, SD = 2.4, $n = 101$), width in locomotion 3.8–9.6 µm (average 6.8 µm, SD = 1.8, $n = 101$), nucleus diameter at widest point 1.7–5.1 µm (average 2.9 µm, SD = 0.8, $n = 88$), average nucleolus diameter 0.6–2.6 µm (average 1.6 µm, SD = 0.4, $n = 88$), and cysts diameter 4.9–9.1 µm (average 7.2 µm, SD = 1.2, $n = 62$). Nucleus and nucleolus commonly round. Primarily a bacterivore.

Type location. Strain Union 16-1-3 of *Kanabo kenzan* n. g. et n. sp. was obtained from crust from sidewalk crack on the Mississippi State University campus in Starkville, Mississippi, USA Lat. 33.455292°, Long. −88.789532°, in May of 2016.

Type material. This type culture (Union 16-1-3) is deposited in a metabolically inactive state with the Culture Collection of Algae and Protozoa (CCAP 2538/1). This culture is also considered the hapantotype (name-bearing type) of the species, under article 73.3 of the International Code of Zoological Nomenclature (ICZN, 1999).

Gene Sequence data. The nearly complete SSU-rRNA gene of the type isolate (Union-16-1-3) is deposited on GenBank under accession MN508059.

ZooBank ID: urn:lsid:zoobank.org:act:61249BB8-80BE-4515-9B0D-E664FD701855.

Etymology. For the specific epithet, we chose "kenzan" referring to the finely tapered subpseudopodia that the amoeba exhibits. A kenzan (n) is a traditional tool used many needles for Japanese flower art, which is a spiked comb with many needles. *Kenzan* is neuter.

Parakanabo Fry & Brown n. g

Diagnosis: A small limax-shaped amoeba, with greater length than breadth, with finely tapered subpseudopodia, generally tubular shape, oftentimes tubular shape in form, with an anterior contractile vacuole, and can form a round, smooth-walled cyst. Rarely, cells form an irregular circular shape. Amoeboid cells in locomotion display characteristics of a limax shape with elongated hyaloplasm and anterior contract vacuole.

Type species: *P. toge*.

ZooBank ID: urn:lsid:zoobank.org:act:D73FDBBE-2D44-479E-ABDB-6D9D5B892AA6.

Etymology. Named similarly to *Kanabo* owing to its nearly identical morphology, with the prefix *Para-* indicating its paraphyletic phylogenetic proximity to *Kanabo*. *Parakanabo* is neuter.

Parakanabo toge Fry & Brown n. sp.

Diagnosis. Length in locomotion 10.3–29.3 μm (average 18.9 μm, SD = 3.1, *n* = 63), width in locomotion 4.2–9.1 μm (average 6.5 μm, SD = 1.1, *n* = 63), nucleus diameter at widest point 2.3–5.5 μm (average 3.8 μm, SD = 0.7, *n* = 20), average nucleolus diameter 1.2–3.3 μm (average 2.1 μm, SD = 0.6, *n* = 20), and cysts diameter 7.6–9.9 μm (average 8.5 μm, SD = 0.6, *n* = 20). Nucleus and nucleolus commonly round. Primarily a bacterivore.

Type location: Strain Harn W-18-15 of *Parakanabo toge* n. g. et n. sp. was obtained from crust from between bricks of the eastern wall of Harned Hall on the Mississippi State University campus in Starkville, Mississippi, USA Lat. 33.455558°, Long. −88.787748°, in August of 2018.

Type material. This type culture (Harn W-18-15) is deposited in a metabolically inactive state with the with the CCAP, CCAP 2557/1. This culture is also considered the hapantotype (name-bearing type) of the species, under article 73.3 of the ICZN (1999).

Gene Sequence data. The nearly complete SSU-rRNA gene of the type isolate (Harn W-18-15) is deposited on GenBank under accession OQ054990.

ZooBank ID. urn:lsid:zoobank.org:act:9CECEADF-C312-4B55-A60F-37805C5AA5C6.

Etymology. For the specific epithet, we chose "toge" referring to the look of the cells with finely tapered pseudopodia resembling a Kanabō weapon, which is a spiked club. Toge (n) is the Japanese word for spike. *Toge* is neuter.

ACKNOWLEDGMENTS

This work was supported by the United States National Science Foundation (NSF) Division of Environmental Biology (DEB) grant 2100888 (http://www.nsf.gov) awarded to MWB. We thank Prof. Ryoma Kamikawa (Kyoto University) with help for Japanese words used for the etymology of our new taxa.

DATA AVAILABILITY STATEMENT

The SSU rRNA gene sequences and the raw Illumina sequencing reads have been deposited on NCBI under the accessions MN508059, OQ054989, OQ054990 and in Bioproject PRJNA1026935, respectively. The transcriptome assemblies, predicted proteins, untrimmed and trimmed SSU alignment, the untrimmed and trimmed single gene alignments, the phylogenomic matrix, and the single ortholog trees are available on Figshare https://doi.org/10.6084/m9.figshare.24492526.

ORCID

Nicholas Fry https://orcid.org/0009-0002-8516-4719
Gabriel A. Schuler https://orcid.org/0000-0002-7666-5733
Robert E. Jones https://orcid.org/0000-0001-5227-4773
Alexander K. Tice https://orcid.org/0000-0002-3128-1867
Matthew W. Brown https://orcid.org/0000-0002-1254-0608

REFERENCES

Adl, S.M., Bass, D., Lane, C.E., Lukeš, J., Schoch, C.L., Smirnov, A. et al. (2018) Revisions to the classification, nomenclature, and diversity of eukaryotes. *The Journal of Eukaryotic Microbiology*, 66, 4–119. Available from: https://doi.org/10.1111/jeu.12691

Berney, C., Geisen, S., Wichelen, J., Nitsche, F., Vanormelingen, P., Bonkowski, M. et al. (2015) Expansion of the 'Reticulosphere': diversity of novel branching and network-forming amoebae helps to define Variosea (Amoebozoa). *Protist*, 166, 271–295. Available from: https://doi.org/10.1016/j.protis.2015.04.001

Blandenier, Q., Seppey, C.V.W., Singer, D., Vlimant, M., Simon, A., Duckert, C. et al. (2017) *Mycamoeba gemmipara* nov. gen., nov. sp., the first cultured member of the environmental Dermamoebidae clade LKM74 and its unusual life cycle. *The Journal of Eukaryotic Microbiology*, 64, 257–265.

Bolger, A.M., Lohse, M. & Usadel, B. (2014) Trimmomatic: a flexible trimmer for Illumina sequence data. *Bioinformatics*, 30, 2114–2120.

Brown, M.W. (2019) Effective and efficient cytoskeleton (actin and microtubules) fluorescence staining of adherent eukaryotic cells v1 (protocols.io.8wkhxcw). https://doi.org/10.17504/protocols.io.8wkhxcw

Brown, M.W., Silberman, J.D. & Spiegel, F.W. (2012) A contemporary evaluation of the acrasids (Acrasidae, Heterolobosea, Excavata). *European Journal of Protistology*, 48(2), 103–123. Available from: https://doi.org/10.1016/j.ejop.2011.10.001

Cavalier-Smith, T. (1998) A revised six-kingdom system of life. *Biological reviews of the Cambridge Philosophical Society*, 73(3), 203–266. https://doi.org/10.1017/s0006323198005167

Cavalier-Smith, T., Chao, E.E.Y. & Oates, B. (2004) Molecular phylogeny of Amoebozoa and the evolutionary significance of the unikont *Phalansterium*. *European Journal of Protistology*, 40, 21–48. Available from: https://doi.org/10.1016/j.ejop.2003.10.001

Clark, K., Karsch-Mizrachi, I., Lipman, D.J., Ostell, J. & Sayers, E.W. (2015) GenBank. *Nucleic Acids Research*, 44, D67–D72.

Geisen, S. & Bonkowski, M. (2018) Methodological advances to study the diversity of soil protists and their functioning in soil food webs. HUMUSICA 3 – rev. *Applied Soil Ecology*, 123, 328–333. Available from: https://doi.org/10.1016/j.apsoil.2017.05.021

Grabherr, M.G., Haas, B.J., Yassour, M., Levin, J.Z., Thompson, D.A., Amit, I. et al. (2011) Full-length transcriptome assembly from RNA-seq data without a reference genome. *Nature Biotechnology*, 29(7), 644–652. Available from: https://doi.org/10.1038/nbt.1883

Griffin, J.L. (1972) Movement, fine structure and fusion of pseudopods of an enclosed amoeba, *Difflugiella* sp. *Journal of Cell Science*, 10, 563–583.

Harding, T., Brown, M.W., Plotnikov, A., Selivanova, E., Park, J.S., Gunderson, J.H. et al. (2013) Amoeba stages in the deepest branching Heteroloboseans, including *Pharyngomonas*: evolutionary and systematic implications. *Protist*, 164, 272–286.

Kang, S., Tice, A.K., Spiegel, F.W., Silberman, J.D., Pánek, T., Cepicka, I. et al. (2017) Between a pod and a hard test: the deep evolution of amoebae. *Molecular Biology and Evolution*, 34(9), 2258–2270.

Katoh, K. & Standley, D.M. (2013) MAFFT multiple sequence alignment software version 7: improvements in performance and usability. *Molecular Biology and Evolution*, 30(4), 772–780. Available from: https://doi.org/10.1093/molbev/mst010

Kudryavtsev, A., Voytinsky, F. & Volkova, E. (2022) *Coronamoeba villafranca* gen. nov. sp. nov. (Amoebozoa, Dermamoebida) challenges the correlation of morphology and phylogeny in Amoebozoa. *Scientific Reports*, 12, 12541. Available from: https://doi.org/10.1038/s41598-022-16721-2

Lahr, D.J.G., Kosakyan, A., Lara, E., Mitchell, E.A.D., Morais, L., Porfirio-Sousa, A.L. et al. (2019) Phylogenomics and morphological reconstruction of Arcellinida testate amoebae highlight diversity of microbial eukaryotes in the Neoproterozoic. *Current Biology*, 29, 991–1001.e3. Available from: https://doi.org/10.1016/j.cub.2019.01.078

Lühe, M. (1913) Erster Band: Protozoa. In: *Handbuch der Morphologie der wirbellosen Tiere*. Jena: G. Fischer, p. 416. Available from: https://www.biodiversitylibrary.org/page/12269925

Mann, D.G. & Evans, K.M. (2008) The species concept and cryptic diversity. Proceedings of the 12th International Conference on Harmful Algae, 262–268. Copenhagen: International Society for the Study of Harmful Algae and Intergovernmental Oceanographic Commission of UNESCO.

Maritz, J.M., Ten Eyck, T.A., Elizabeth Alter, S. & Carlton, J.M. (2019) Patterns of protist diversity associated with raw sewage in New York City. *The ISME Journal*, 13, 2750–2763. Available from: https://doi.org/10.1038/s41396-019-0467-z

McKinney, M.L. (2002) Urbanization, biodiversity, and conservation: the impacts of urbanization on native species are poorly studied, but educating a highly urbanized human population about these impacts can greatly improve species conservation in all ecosystems. *BioScience*, 52, 883–890. Available from: https://doi.org/10.1641/0006-3568(2002)052[0883:UBAC]2.0.CO;2

Minh, B.Q., Schmidt, H.A., Chernomor, O., Schrempf, D., Woodhams, M.D., von Haeseler, A. et al. (2020) IQ-TREE 2: new models and efficient methods for phylogenetic inference in the genomic era. *Molecular Biology and Evolution*, 37, 1530–1534.

Nikolaev, S.I., Mylnikov, A.P., Berney, C., Fahrni, J., Pawlowski, J., Aleshin, V.V. et al. (2004) Molecular phylogenetic analysis places *Percolomonas cosmopolitus* within Heterolobosea: evolutionary implications. *The Journal of Eukaryotic Microbiology*, 51, 575–581.

Olive, L.S. (1964) A new member of the Mycetozoa. *Mycologia*, 56, 885–896.

Olive, L.S. & Stoianovitch, C. (1971) *Planoprotostelium*, a new genus of Protostelids. *Journal of the Elisha Mitchell Scientific Society*, 87, 115–119.

Pánek, T., Eliáš, M., Vancová, M., Lukeš, J. & Hashimi, H. (2020) Returning to the fold for lessons in mitochondrial crista diversity and evolution. *Current Biology*, 30, R575–R588.

Picelli, S., Faridani, O.R., Björklund, Å.K., Winberg, G., Sagasser, S. & Sandberg, R. (2014) Full-length RNA-seq from single cells using smart-seq2. *Nature Protocols*, 9, 171–181.

Ramirez, K.S., Leff, J.W., Barberán, A., Bates, S.T., Betley, J., Crowther, T.W. et al. (2014) Biogeographic patterns in below-ground diversity in New York City's Central Park are similar to those observed globally. *Proceedings of the Royal Society B: Biological Sciences*, 281, 20141988.

Ronquist, F., Teslenko, M., Mark, P., Ayres, D.L., Darling, A., Hohna, S. et al. (2012) MrBayes 3.2: efficient Bayesian phylogenetic inference and model choice across a large model space. *Systematic Biology*, 61, 539–542. Available from: https://doi.org/10.1093/sysbio/sys029

Shadwick, J.D.L., Silberman, J.D. & Spiegel, F.W. (2018) Variation in the SSUrDNA of the genus *Protostelium* leads to a new phylogenetic understanding of the genus and of the species concept for *Protostelium mycophaga* (Protosteliida, Amoebozoa). *The Journal of Eukaryotic Microbiology*, 65, 331–344. Available from: https://doi.org/10.1111/jeu.12476

Shadwick, L.L., Spiegel, F.W., Shadwick, J.D., Brown, M.W. & Silberman, J.D. (2009) Eumycetozoa = Amoebozoa?: SSUrDNA phylogeny of protosteloid slime molds and its significance for the amoebozoan supergroup. *PLoS One*, 4(8), e6754. Available from: https://doi.org/10.1371/journal.pone.0006754

Smirnov, A., Nassonova, E., Geisen, S., Bonkowski, M., Kudryavtsev, A., Berney, C. et al. (2017) Phylogeny and systematics of Leptomyxid amoebae (Amoebozoa, Tubulinea, Leptomyxida). *Protist*, 168, 220–252. Available from: https://doi.org/10.1016/j.protis.2016.10.006

Smirnov, A.V., Chao, E., Nassonova, E.S. & Cavalier-Smith, T. (2011) A revised classification of naked lobose amoebae (Amoebozoa: lobosa). *Protist*, 162, 545–570. Available from: https://doi.org/10.1016/j.protis.2011.04.004

Spiegel, F.W., Gecks, S.C. & Feldman, J. (1994) Revision of the genus *Protostelium* (Eumycetozoa) I: the *Protostelium mycophaga* group and the *P. irregularis* group. *The Journal of Eukaryotic Microbiology*, 41(5), 511–518. Available from: https://doi.org/10.1111/j.1550-7408.1994.tb06051.x

Spiegel, F.W., Shadwick, L.L., Ndiritu, G.G., Brown, M.W., Aguilar, M. & Shadwick, J.D. (2017) Protosteloid Amoebae (Protosteliida, Protosporangiida, Cavosteliida, Schizoplasmodiida, Fractoviteliida, and Sporocarpic Members of Vannellida, Centramoebida, and Pellitida). In: Archibald, J., Simpson, A.G.B., Slamovits, C.H., Margulis, L., Melkonian, M., Chapman, D.J. et al. (Eds.) *Handbook of the protists*. Cham: Springer. Available from: https://doi.org/10.1007/978-3-319-32669-6_12-1

Stamatakis, A. (2014) RAxML version 8: a tool for phylogenetic analysis and post-analysis of large phylogenies. *Bioinformatics*, 30, 1312–1313.

Tekle, Y.I., Wang, F., Wood, F.C., Anderson, O.R. & Smirnov, A. (2022) New insights on the evolutionary relationships between the major lineages of Amoebozoa. *Scientific Reports*, 12(1), 11173. Available from: https://doi.org/10.1038/s41598-022-15372-7

Tice, A.K., Shadwick, L.L., Fiore-Donno, A.M., Geisen, S., Kang, S., Schuler, G.A. et al. (2016) Expansion of the molecular and morphological diversity of Acanthamoebidae (Centramoebida, Amoebozoa) and identification of a novel life cycle type within the group. *Biology Direct*, 11, 69. Available from: https://doi.org/10.1186/s13062-016-0171-0

Tice, A.K., Spiegel, F.W. & Brown, M.W. (2023) Phylogenetic placement of the protosteloid amoeba Microglomus paxillus identifies another case of sporocarpic fruiting in Discosea (Amoebozoa). *The Journal of eukaryotic microbiology*, 70(4), e12971. Available from: https://doi.org/10.1111/jeu.12971

Tice, A.K., Žihala, D., Pánek, T., Jones, R.E., Salomaki, E.D., Nenarokov, S. et al. (2021) PhyloFisher: a phylogenomic package for resolving eukaryotic relationships. *PLoS Biology*, 19, e3001365.

Volkova, E. & Kudryavtsev, A. (2021) A morphological and molecular reinvestigation of *Janickina pigmentifera* (Grassi, 1881) Chatton 1953 – an amoebozoan parasite of arrow-worms (Chaetognatha). *International Journal of Systematic and Evolutionary Microbiology*, 71, 005094.

Walthall, A.C., Tice, A.K. & Brown, M.W. (2016) A new species of *Flamella* (Amoebozoa, Variosea, Gracilipodida) isolated from a freshwater pool in southern Mississippi, USA. *Acta Protozoologica*, 55, 111–117.

Journal of Eukaryotic Microbiology ISOP Published by the International Society of Protistologists

Wichelen, J.V., D'Hondt, S., Claeys, M., Vyverman, W., Berney, C., Bass, D. et al. (2016) A hotspot of amoebae diversity: 8 new naked amoebae associated with the planktonic bloom-forming cyanobacterium *Microcystis*. *Acta Protozoologica*, 55, 61–87.

SUPPORTING INFORMATION

Additional supporting information can be found online in the Supporting Information section at the end of this article.

How to cite this article: Fry, N., Schuler, G.A., Jones, R.E., Kooienga, P.G., Jira, V., Shepherd, M. et al. (2024) Living in the cracks: Two novel genera of Variosea (Amoebozoa) discovered on an urban sidewalk. *Journal of Eukaryotic Microbiology*, 71, e13020. Available from: https://doi.org/10.1111/jeu.13020